



Conjugate nonlinear-optical loop mirror (Conj-NOLM)-based phase-preserving multilevel amplitude regenerator

FENG WEN,^{1,2,*} BAOJIAN WU,¹ KUN QIU,¹ AND STYLIANOS SYGLETOS²

¹Key Lab of Optical Fiber Sensing and Communication Networks, Ministry of Education, University of Electronic Science and Technology of China, Chengdu 611731, China

²Aston Institute of Photonic Technologies, Aston University, Birmingham B4 7ET, UK

*fengwen@uestc.edu.cn

Abstract: We propose a novel phase-preserving multilevel amplitude regenerator scheme by cascading two nonlinear-optical loop mirrors (NOLMs) with an intermediate optical phase conjugator (OPC) stage. Joint parameter optimization of the two NOLM units has been carried out to cancel the introduced phase distortion and enable a more power-efficient performance. Moreover, our scheme combines the operation of the NOLM and the OPC in a single subsystem, enabling the compensation of both amplitude and phase distortions when located symmetrically in a transmission link. To this end, extensive numerical simulations have been performed to evaluate the regeneration performance in a transmission link dominated by amplified spontaneous emission (ASE) noise and Kerr-induced nonlinear distortions (self-phase modulation-induced phase distortion), achieving over 100% reach extension compared to the cases of un-regenerative, or a mid-span OPC-based transmission links.

Published by The Optical Society under the terms of the [Creative Commons Attribution 4.0 License](https://creativecommons.org/licenses/by/4.0/). Further distribution of this work must maintain attribution to the author(s) and the published article's title, journal citation, and DOI.

1. Introduction

Advanced modulation formats have found a commercial application in optical communication systems as they can bring significant increase of the fiber link capacity. However, at high constellation orders transmitted signals become more vulnerable to amplified spontaneous emission (ASE) and fiber nonlinearity induced degradations [1]. All-optical regenerators represent a promising technology to combat those effects directly in the optical domain, avoiding the use of complex and power consuming optical-electrical-optical (O-E-O) conversions [2]. Although schemes that can even support multi-wavelength operation have been proposed [3–5], they mostly deal with single amplitude level formats. To meet the requirements of highly-spectral-efficient signals regenerators that can support multilevel operation in the amplitude domain are required. In recent years, fiber-based nonlinear-optical loop mirrors (NOLMs) have been intensively investigated as promising candidates for multilevel amplitude regeneration [6–9] due to their oscillatory amplitude transfer function. However, a challenging design issue in their development is the mitigation of the nonlinear phase distortion they introduce to the input signals due to the self-phase modulation (SPM) effects in the highly nonlinear fiber (HNLF). Even for signals of pure amplitude-shift keying (ASK) modulation, the development of nonlinear phase distortion will degrade the transmission reach due to the Gordon-Mollenauer effect [10].

Up to date, mitigation of the nonlinear phase distortion and achievement of phase preserving operation in a single-NOLM based regenerator has been achieved through the design of a highly asymmetric interferometer scheme, enabled either with the use of a simple attenuator [6], or a bidirectional attenuator [7,11], or a bidirectional Erbium-doped fiber amplifier (Bi-EDFA) [8,12,13]. Those single-NOLM asymmetric schemes could enable the

interference of two highly unequal in amplitude counter-propagating waves at the output coupler, for regenerative amplitude response and a phase transparent operation. No matter where the extra loss or gain was applied in the interferometer high power signals were naturally expected at the input, jeopardizing the power efficiency of the scheme. Furthermore, stimulated Brillouin and Raman scattering (SBS, SRS) effects in the HNLf constitute major preventing factors of multilevel amplitude response.

In this paper we introduce a novel phase-preserving setup by cascading two NOLMs with an intermediate optical phase conjugator (OPC) to enable power-efficient multilevel amplitude regeneration. The NOLM units have been jointly optimized to enable operation at significantly lower input power levels compared to a single-NOLM scheme. At the same time, the use of the mid-span OPC cancels their introduced nonlinear phase distortion. Extensive optimization of the various subsystem parameters has been performed to maximize overall performance. Moreover, we have investigated the operation of our proposed scheme as a mid-span element in the transmission link, demonstrating over 100% reach extension compared to the un-regenerative case or the use of a mid-span OPC only in the link. The rest of the paper is organized as follows: in Section 2 we introduce the theoretical model of the proposed Conj-NOLM regenerator and perform the joint optimization of its parameters; in Section 3 we investigate the phase and amplitude response and perform comparison with the traditional single-NOLM scheme; in Section 4 we investigate the regenerative performance in cascaded transmission for 16-level quadrature amplitude modulation (16-QAM) signals; and finally, in Section 5, we draw the conclusions of our study.

2. Theoretical model

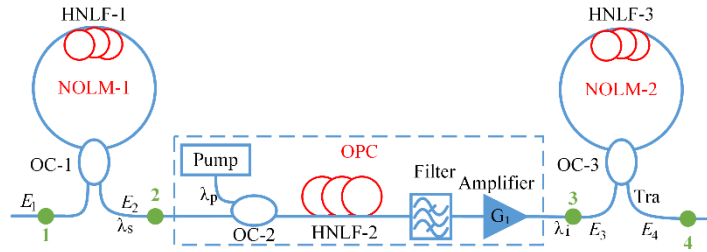


Fig. 1. Proposed Conj-NOLM regenerator subsystem.

The proposed conjugate NOLM (Conj-NOLM) regenerator comprising two NOLM units connected by an intermediate OPC stage, is depicted in Fig. 1. For the modelling of the subsystem only the forward propagating light was taken into account ignoring any other backward light reflection. An input signal E_1 , centered at λ_s , entered the first NOLM and was split into two counter-propagating waves, which acquired a nonlinear phase difference due to the high asymmetry of the interferometer. The resulted wave E_2 , at the output of the 1st-NOLM, i.e. monitoring point-2, can be written as [14]:

$$E_2 = C_1 \left[\overline{\beta}_1 \exp(i\overline{\beta}_1\theta_1) - \beta_1 \exp(i\beta_1\theta_1) \right] E_1 \quad (1)$$

where the loss factor is $C_1 = \exp(-\alpha_1 L_1 / 2)$, and the nonlinear phase factor is $\theta_1 = \gamma_1 P_1 L_1$; α_1 , L_1 and γ_1 are respectively the fiber loss, length and nonlinear coefficient of the highly nonlinear fiber (HNLf-1) in the NOLM-1 unit; $P_1 = |E_1|^2$ is input signal power; β_1 is the amplitude splitting ratio of the optical coupler (OC-1), and $\overline{\beta}_1 = 1 - \beta_1$. This experimentally verified NOLM model [14] considered only the SPM as the major effect and ignored other nonlinear influences from the counter propagation of the signal waves. Equation (1) reveals not only the well-known oscillatory behavior in the amplitude transfer function of the NOLM,

but also the introduced nonlinear phase modulation, through the $\exp(i\beta_1\theta_1)$ and $\exp(i\bar{\beta}_1\theta_1)$ terms, which can be a source of severe signal distortion.

Subsequently, the transmitted signal E_2 was coupled into the highly nonlinear fiber (HNLF-2) of the OPC unit where it interacted through four-wave mixing (FWM) with a strong continuous-wave (CW) light at λ_p , creating a conjugated signal at λ_i , which was selected by an optical filter and boosted by an optical amplifier of gain G_1 , resulting in:

$$E_3 = \sqrt{G_1}\eta E_2^* \quad (2)$$

where η is the conversion efficiency of the FWM process. The optical amplifier worked only as power compensator, without introducing ASE noise, which allowed us to focus only on the influence of the nonlinear effects. The same assumption was also considered for the mid-span OPC links in the study of Section 4 to enable a fair comparison. The conjugated signal was subsequently launched into the second NOLM unit (NOLM-2), giving at its transmission output:

$$E_4 = C_2 \sqrt{G_1}\eta \left[\bar{\beta}_1 \exp(-i\bar{\beta}_1\theta_1) - \beta_1 \exp(-i\beta_1\theta_1) \right] \left[\bar{\beta}_2 \exp(i\bar{\beta}_2\theta_2) - \beta_2 \exp(i\beta_2\theta_2) \right] E_1^* \quad (3)$$

where $C_2 = \exp\left(-\frac{\alpha_1 L_1 + \alpha_2 L_2}{2}\right)$ is the loss factor; $\theta_2 = \gamma_2 P_3 L_2$ represents the nonlinear phase shift; α_2 , L_2 and γ_2 are the fiber loss, length and nonlinear coefficient of the HNLF-3 in the NOLM-2 unit, respectively; β_2 is the amplitude splitting ratio of the optical coupler (OC-3), and $\bar{\beta}_2 = 1 - \beta_2$; P_3 is the optical power of the boosted idler signal (monitoring point 3) $P_3 = G_1 \eta^2 \exp(-\alpha_1 L_1) [1 - 2\beta_1(1 - \beta_1)(1 - \cos\phi_1)] P_1$, and the phase shift is $\phi_1 = (2\beta_1 - 1)\gamma_1 P_1 L_1$. Equation (3) governed the total output of the proposed two-NOLM cascaded subsystem that is depicted in Fig. 1, including both nonlinear amplitude and phase responses.

For phase-preserving operation, we must eliminate the influence of the power-dependent phase-shift terms on the output signal with the help of the mid-span spectral inversion. One thought would be to enable a power symmetry condition of $P_3 = P_1$ within the Conj-NOLM subsystem, since it would lead to an output signal form of:

$$E_4' = \exp(-\alpha L) \sqrt{G_1}\eta [1 - 2\beta(1 - \beta) \cos\phi] E_1^* \quad (4)$$

with no remaining power-dependent phase shift terms. However, such approach is unrealistic because it sets as requirement the mid-stage optical amplifier to compensate the instantaneous nonlinear amplitude response of the 1st NOLM unit. In other words, the amplifier gain $G_1 = 1/\eta^2 \exp(-\alpha L) [1 - 2\beta(1 - \beta)(1 - \cos\phi)]$, would have to follow the instantaneous variation imposed by modulated phase ϕ , as a result of the SPM effect in the HNLF of the interferometer.

A realistic solution for us was to redesign the 1st NOLM for having an almost linear amplitude response and to achieve compensation of its nonlinear phase shift with the help of the OPC and the subsequent 2nd NOLM unit. This allowed the use of an optical amplifier of constant-gain. The main subsystem optimization parameters were the amplitude splitting ratio β_1 of the 1st-NOLM and the net gain $\varepsilon = G_1 \eta^2 \exp(-\alpha_1 L_1)$ defining the signal power level after 1st NOLM and the OPC stage, i.e. at the input of the 2nd NOLM. For simplification, the HNLF parameters in the two NOLM units, and the OPC were similar to those reported in the experiment of [14]: the nonlinear coefficient γ was $7\text{W}^{-1}/\text{km}$, the total loss was 12dB and the

fiber length L was 606m. The amplitude splitting ratio β_2 of the 2nd-NOLM was chosen to be 0.95, which enabled an effective amplitude noise suppression. The optimization procedure had the following steps: we firstly increased the input amplitude $|E_1|$ from 0 to $2.2\sqrt{W}$, to support operation at the targeted number of amplitude levels, in our case three-levels corresponding to 16-QAM signals. Then, using (3) we calculated the phase change $\Delta\varphi = \varphi_{\max} - \varphi_{\min}$ (in degrees) of the output signal E_4 , where φ_i ($i = \max$ or \min) was the maximum or minimum phase achieved in the aforementioned amplitude range. Obviously, we had to identify the operational conditions enabling minimization of the phase change $\Delta\varphi$. Figure 2 depicts the dependence of the phase change $\Delta\varphi$ (in degrees) to the net gain ε and the amplitude splitting ratio β_1 . For most of the input values, the calculated phase change $\Delta\varphi$ could reach 360° , see the red-colored regions, as a result of the high operational powers required for multilevel performance. On the contrary, $\Delta\varphi$ could be significantly reduced when the signal was amplified, i.e. $\varepsilon \geq 1$, and the splitting ratio β_1 became close to 1. The minimum phase change of 8.8° was achieved for $\varepsilon = 1.056$ and $\beta_1 = 0.999$, see red point, which corresponded to a highly asymmetrical NOLM structure with an almost linear amplitude response. We also note that our design is highly sensitive to the splitting ratio β_1 of the 1st NOLM, since small deviations from the optimum value can give rise to large residual phase changes at the output of the regenerator. Nevertheless, highly asymmetric couplers of 99.9:0.1 splitting ratio across the whole C-band are commercially available [15] to support our scheme and they have been already used in other experimental demonstrations, such as cavity ring down spectroscopy [16] and optical phased arrays [17].

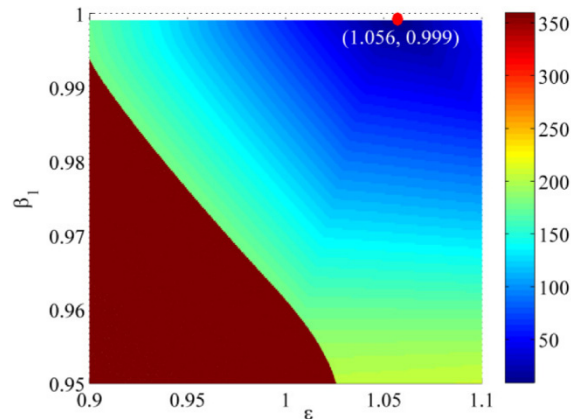


Fig. 2. Dependence of the phase change $\Delta\varphi$ on the net gain ε and the splitting ratio β_1 .

3. Phase and amplitude responses

Having optimized the structure of the Conj-NOLM scheme, we examined more thoroughly the phase evolution as a function of the amplitude level for the input signal at the different stages of the regenerator subsystem for achieving the phase-preserving operation. We also investigated the overall amplitude transfer function optimized for 16-QAM operation and we performed comparison with a traditional phase-preserving regeneration scheme [6].

3.1. Phase response

Figure 3(a) depicts the phase evolution of the signals at the monitoring points (MPs) 2-4 as a function of the input amplitude $|E_1|$ when the input amplitude level varied from 0 to $2.2\sqrt{W}$, covering the operational range of the three-level amplitude regenerator. With the increase of the input level, a large counter-clockwise phase rotation $\Delta\varphi$ of up to 360° was observed at the

output of the 1st-NOLM, see the blue dash line. Although in a conventional NOLM regenerator this nonlinear phase rotation would have been highly detrimental, in our case, it worked only as a pre-distortion to be cancelled in the subsequent stages. Indeed, the OPC reversed the sign of the nonlinear phase shift (black line), whereas the 2nd-NOLM unit reduced the phase change to only 8.8°.

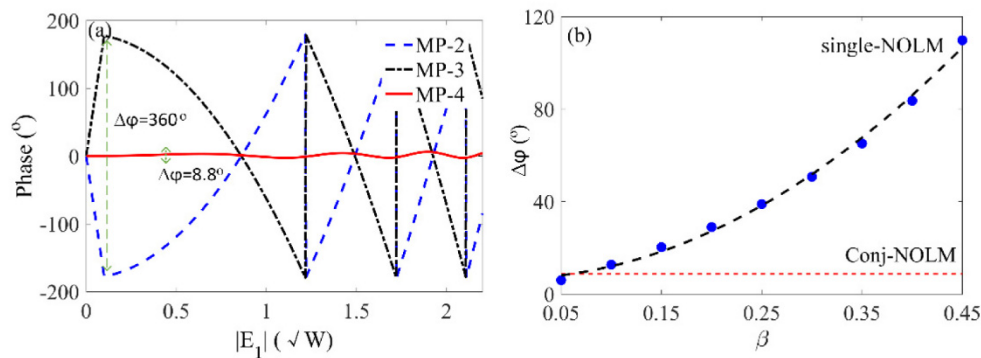


Fig. 3. (a) Phase evolution of the output signals from monitoring points 2-4 with the increase of the input amplitude $|E_1|$, and (b) minimum phase change $\Delta\phi$ achieved for different splitting ratios β in the single-NOLM asymmetric scheme.

Subsequently, we performed comparison of our proposed Conj-NOLM scheme with the traditional single-NOLM asymmetric scheme [6], in terms of introduced nonlinear phase change $\Delta\phi$ on the output signals. In the single-NOLM asymmetric scheme, an extra loss factor required in the interferometer (e.g. through an optical attenuator) to reverse the power levels of two counter-propagating signals before the HNLF for minimizing the nonlinear phase distortion on the output signal. Thus, the residual phase change $\Delta\phi$ depended on this extra loss factor, as well as, the amplitude splitting ratio β of the optical coupler at the NOLM output. We used the same definition of the phase change $\Delta\phi$, which represented the phase variation in a three-level amplitude regenerator, to compare the phase-preserving performance between two schemes. Figure 3(b) shows the calculated $\Delta\phi$ for the single-NOLM asymmetric scheme, as a function of the amplitude splitting ratio β . Each depicted $\Delta\phi$ corresponded to the minimum phase change identified by varying the extra loss in the branch of the NOLM. For comparison, we calculated also the nonlinear phase shift of the output signal when using the proposed Conj-NOLM scheme. The lowest $\Delta\phi$ was achieved for the most asymmetric structure, i.e. with the lowest splitting ratio. Specifically, a very low phase change, similar to our proposed scheme, could be theoretically obtained when the amplitude splitting ratio β was close to 0.05. However, this operation point required an additional loss of ~ 45 dB in the branch of the single-NOLM, which would detrimentally affect the power efficiency and the sensitivity of the regenerator. On the contrary, no additional loss was used in the Conj-NOLM scheme. For a more moderate splitting ratio value of $\beta = 0.15$ and an extra loss of 20dB, experimentally reported in [6] we calculated for the single-NOLM scheme a residual phase change 55.28° (the same residual phase level can also be found in the single-NOLM scheme with a bidirectional EDFA [8,13]), i.e. six times larger than with our scheme. Obviously, our proposed Conj-NOLM regenerator demonstrates a much better phase-preserving performance.

3.2. Amplitude response

Figure 4(a) depicts the nonlinear amplitude response for the Conj-NOLM and the single-NOLM, respectively. The figure confirms the almost linear amplitude response of the first NOLM due to its highly asymmetric structure, see green line. Nevertheless, the second NOLM could still enable an oscillatory response with three plateau regions at its output, see

red line. The efficiency of the achieved noise suppression depended on the amplitude splitting ratio β_2 of the 2nd-NOLM but also required a joint optimization of the amplitude splitting ratio β_1 and the net gain \mathcal{E} as discussed in Section 2. We also plot the amplitude response of the single-NOLM scheme, see the blue dot-dash line in Fig. 4(a), for a splitting ratio of $\beta = 0.15$ and an extra loss of 20dB for enabling phase preserving operation [6]. Because of this extra loss the operational power of each regenerative level was significantly increased. In particular, the third regenerative level in the single-NOLM case required 8.15dB more input power compared to our Conj-NOLM scheme. Accordingly, the output power of the single-NOLM was significantly lower. Although not shown in the normalized curves of Fig. 4(a), we calculated 12 dB less output power for the third regenerative level in the single-NOLM case compared to our scheme. This power difference is expected to become even higher when the extra loss in the single-NOLM scheme increases to 45dB to reach the 8.8° degrees residual phase shift level of our regenerator. These results suggest better power operational characteristics for the Conj-NOLM regenerator with less impact on the signal-to-noise ratio degradation along the link.

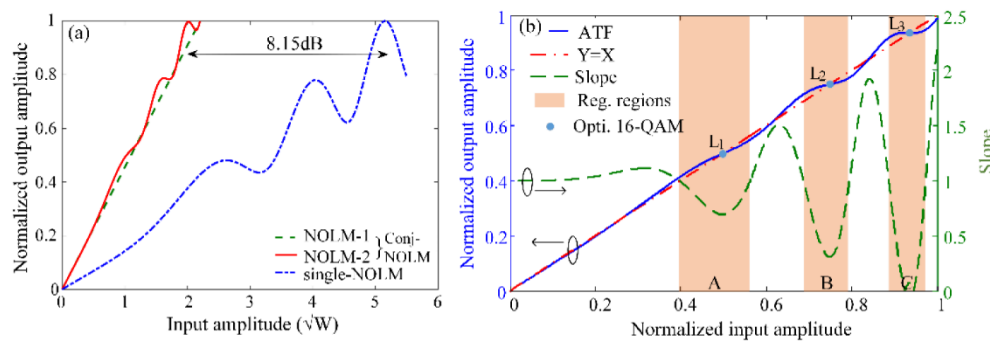


Fig. 4. (a) Nonlinear amplitude transfer functions that achieved by the two NOLM units in the Conj-NOLM regenerator and the single-NOLM scheme, (b) normalized amplitude transfer curve of the Conj-NOLM regenerator and the optimized alphabets of 16-QAM signals.

Figure 4(b) depicts the overall nonlinear transfer function of the Conj-NOLM regenerator. The transfer function has been normalized with respect to a line that crosses the plateau regions at the local-minimum slope points. The cross points L_1 , L_2 , L_3 of the normalized amplitude transfer curve (ATF) and the $Y = X$ line, labeled in Fig. 4(b), are the stationary points of this nonlinear transformation which in a cascaded operation should remain unchanged. Therefore, they should define the alphabet positions for an input 16-QAM signal. The green line in Fig. 4(b) depicts the calculated slope of the transfer function curve, defining for absolute values less than 1 the regenerative regions of our subsystem. These are shown by the three pink-colored areas A to C depicted with a more effective noise suppression being achieved at the center of each of them.

4. Transmission link evaluation

In this section we present the results of the performance evaluation of the Conj-NOLM regenerator in transmission link of N cascaded regenerative sections, see Fig. 5, and we compare with the bypass, i.e. un-regenerative case, and the case of using a mid-span OPC in the link. As we wanted to focus on the relative impact of the main transmission effects on the performance of our regenerator we considered two hypothetical transmission scenarios. In the first scenario we considered transmission in the linear regime by ignoring any nonlinearity in the fiber link and taking into account only the ASE noise generated by the optical amplifiers. In the second scenario, we took into account also the nonlinear phase distortion that is generated along the transmission system due to Kerr-effect induced signal-signal and signal-noise interactions. No dispersion effects were taken into account, i.e. signal transmission

assumed in the zero-dispersion wavelength. The Conj-NOLM regenerator or the OPC module were placed in the middle of each of those section, whereas fiber spans before and after the regenerator introduced the nonlinear phase distortion of $\varphi_{NL} = \gamma L_{eff} P_s = 28P_s$ in which P_s was the instantaneous power of each symbol whereas the ASE noise was added separately at the input of each transmission fiber.

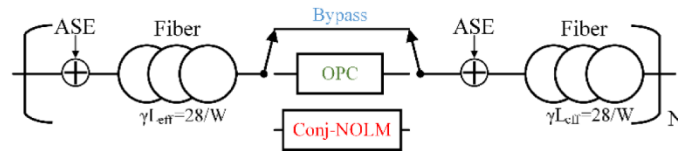


Fig. 5. Transmission evaluation in the un-regenerative, the mid-span OPC and the Conj-NOLM links.

4.1. Impact of ASE only noise

ASE noise is generated by EDFAs in the link and introduces both amplitude and phase distortions on the transmitted signal. The only effective way to mitigate this effect and extend the transmission reach is to suppress it through a nonlinear signal regeneration process [3–9]. Here we evaluate the capability of our proposed Conj-NOLM regenerator to provide transmission reach extension against ASE induced degradations for the case of 16-QAM signals.

Following the approach of [18,19] the constellation shape of the input signal was optimized to meet the exact transfer function characteristics of our regenerator. That is, we shifted the amplitude levels of a rectangular 16-QAM according to the alphabets defined in the amplitude transfer curve, see the blue points L_1 to L_3 in Fig. 4(b). The obtained constellation diagram is depicted with dark points in the inset of Fig. 6(a). Subsequently, we launched the 16-QAM signal into a long-haul transmission link of N cascaded (regenerative or OPC only) sections and calculated the bit-error rate (BER) as a function of N . The ASE noise was modelled as additive white Gaussian noise of an average power level defined by a specific signal-to-noise ratio (SNR). Figure 6(a) shows plots of the BER curve as we increase the number N of cascaded transmission sections, and assuming the same loaded noise of SNR = 25dB for each transmission section. When placing the Conj-NOLM subsystem in the middle of the transmission link it reduced substantially the noise accumulation and achieved a reach extension of up to 72.4% compared to the un-regenerative link at the FEC limit (BER = 1.9×10^{-2}). The use of a mid-span OPC link had the same performance with the un-regenerative link case since the OPC is not introducing any suppression of the random noise. The inset of Fig. 6(a) shows also the corresponding constellations with and without the use of the proposed regenerator. Clear amplitude noise suppression is observed on multiple level without any extra phase distortion from the regenerator. The result confirms that the proposed Conj-NOLM scheme enables a phase-preserving multilevel amplitude regeneration performance in long-haul transmission links.

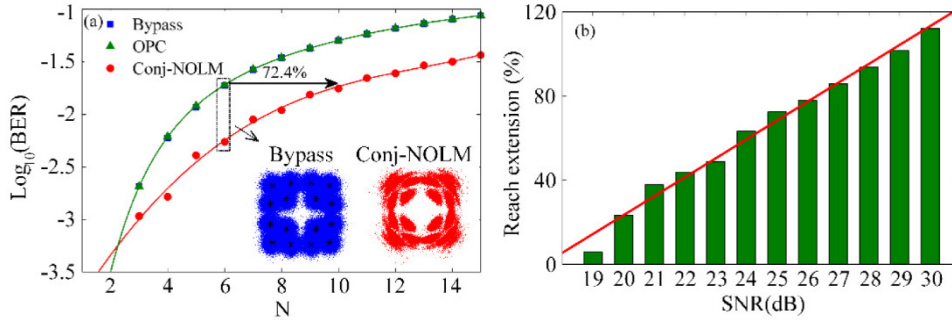


Fig. 6. (a) BER evolutions with the cascaded number N for the un-regenerative link, the mid-span OPC link and the Conj-NOLM link; (b) dependence of the reach extension on the ASE noise strength.

Moreover, we calculated the reach extension as a function of the noise strength, see Fig. 6(b). The reach extension was improving for higher SNR levels due to the more efficient noise suppression achieved around the optimized alphabet points. Specifically, about 110% reach extension was calculated for $\text{SNR} = 30\text{dB}$. With the increase of the noise strength, the performance was degraded because of the limited noise-suppression efficiency of the regenerator. A linear fitting on the reach extension results revealed a 9% improvement per dB increase of the SNR. The transmission performance of the link can be even further improved by enabling also a phase noise suppression, e.g. through the use of phase sensitive amplifiers (PSAs) [20–22].

4.2. ASE noise and nonlinear phase distortion

The next step was to consider, apart from the ASE noise, also the impact of Kerr nonlinearity in the transmission fiber. To this end, we considered the same ASE noise strength ($\text{SNR} = 25\text{dB}$ and $N = 5$) and kept a fixed launched optical power at 5dBm . Figures 7(a) and 7(b) depict the amplitude and phase histograms for the bypass, the mid-span OPC and the Conj-NOLM cases, respectively. In Fig. 7(a), three discrete amplitude levels are observed for the Conj-NOLM link case, due to the achieved noise suppression at the corresponding signal levels. Moreover, we obtain the same phase results after the OPC link or the Conj-NOLM link, see Fig. 7(b), which is a clear evidence that the mid-span spectral inversion in the Conj-NOLM regenerator performs also compensation of the accumulated phase distortion along the fibre transmission link. This suggest also that we can successfully combine the operations of the OPC and NOLM elements in a single subsystem.

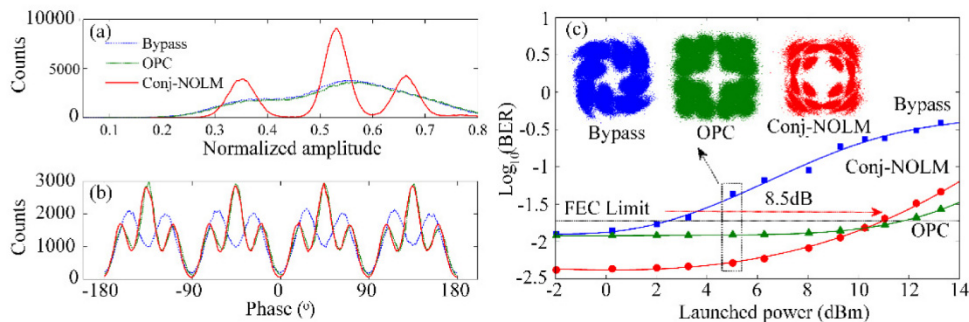


Fig. 7. (a) Amplitude and (b) phase histograms of the un-regenerative, the OPC and the Conj-NOLM cases, and (c) BERs vs. launched optical powers for the bypass, the OPC and the Conj-NOLM cases, and constellations results obtained at 5dBm .

The transmission performance, characterized by BER vs. launched power, is depicted in Fig. 7(c). In the bypass case, the BER results degrade with launched optical powers due to the SPM-induced nonlinear phase distortion, and a BER of 1.9×10^{-2} is calculated for a launched power of 2.4dBm. Placing a mid-link OPC compensated the nonlinear distortion and enabled a BER improvement only at high launched power levels. When including the proposed Conj-NOLM regenerator in the link, we can improve the BER results at all power points. This also allowed for an 8.5dB increase in the launched power, which can correspond to a significant improvement in the total transmission reach. The comparison of the constellation diagrams, taken at 5dBm, among the bypass, OPC and Conj-NOLM cases (Fig. 7(c) inset) further confirms this conclusion. We can see that the use of the regenerator enables a significant reduction of both amplitude and phase distortions. The slightly worse BER performance, observed for a very high launched power in the Conj-NOLM link, may be due to residual phase distortions in the NOLM units and accumulated in the long-haul transmission, which can be improved with the use of PSAs in the link.

5. Conclusion

We have proposed a Conj-NOLM regenerator subsystem, which combines two NOLM units with an intermediate OPC stage, enabling a phase-preserving multilevel amplitude regeneration. The scheme can minimize the NOLM-induced phase distortion down to 8.8° , six times lower than previously reported single-NOLM based regenerator structures. Moreover, our scheme makes an effective utilization of the input signal power to enable multilevel noise suppression performance. By placing the Conj-NOLM in the transmission link, over 100% reach extension was achieved by suppressing the signal's amplitude noise. When considering both of the ASE noise and the nonlinear phase distortion in the transmission link, the regenerator showed that it can reduce the amplitude and phase distortions enabling an 8.5dB increase in the launched power margin which suggests a significant improvement in terms of transmission reach.

Funding

National Natural Science Foundation of China (NSFC) (61505021, 61671108); EPSRC project TRANSNET (EP/R035342/1); Marie Skłodowska-Curie actions (701770-INNOVATION); General Project of Sichuan Provincial Education Department (18ZB0235); 111 Project (B14039).

References

1. A. Carena, V. Curri, P. Poggiolini, G. Bosco, and F. Forghieri, "Maximum reach versus transmission capacity for Terabit superchannels based on 27.75-GBaud PM-QPSK, PM-8QAM, or PM-16QAM," *IEEE Photonics Technol. Lett.* **22**(11), 829–831 (2010).
2. E. Willner, S. Khaleghi, M. R. Chitgarha, and O. F. Yilmaz, "All-optical signal processing," *J. Lightwave Technol.* **32**(4), 660–680 (2014).
3. F. Parmigiani, L. Provost, P. Petropoulos, D. J. Richardson, W. Freude, J. Leuthold, A. D. Ellis, and I. Tomkos, "Progress in multichannel all-optical regeneration based on fiber technology," *IEEE J. Sel. Top. Quantum Electron.* **18**(2), 689–700 (2012).
4. X. Y. Zhou, B. J. Wu, F. Wen, H. C. Zhang, H. Zhou, and K. Qiu, "Total data rate of multi-wavelength 2R regenerators for time-interleaved RZ-OOK signals," *Opt. Express* **22**(19), 22937–22951 (2014).
5. L. Li, P. G. Patki, Y. B. Kwon, V. Stelmakh, B. D. Campbell, M. Annamalai, T. I. Lakoba, and M. Vasilyev, "All-optical regenerator of multi-channel signals," *Nat. Commun.* **8**(1), 884 (2017).
6. T. Roethlingshoefer, T. Richter, C. Schubert, G. Onishchukov, B. Schmauss, and G. Leuchs, "All-optical phase-preserving multilevel amplitude regeneration," *Opt. Express* **22**(22), 27077–27085 (2014).
7. M. Sorokina, S. Sygletos, A. Ellis, and S. Turitsyn, "Regenerative Fourier transformation for dual-quadrature regeneration of multilevel rectangular QAM," *Opt. Lett.* **40**(13), 3117–3120 (2015).
8. T. Roethlingshoefer, G. Onishchukov, B. Schmauss, and G. Leuchs, "Cascaded phase-preserving multilevel amplitude regeneration," *Opt. Express* **22**(26), 31729–31734 (2014).
9. F. Wen, C. P. Tsekrekos, Y. Geng, X. Zhou, B. Wu, K. Qiu, S. K. Turitsyn, and S. Sygletos, "All-optical multilevel amplitude regeneration in a single nonlinear optical loop mirror," *Opt. Express* **26**(10), 12698–12706 (2018).

10. J. P. Gordon and L. F. Mollenauer, "Phase noise in photonic communications systems using linear amplifiers," *Opt. Lett.* **15**(23), 1351–1353 (1990).
11. G. Striegler, M. Meissner, K. Cvecek, K. Sponsel, G. Leuchs, and B. Schmauss, "NOLM-based RZ-DPSK signal regeneration," *IEEE Photonics Technol. Lett.* **17**(3), 639–641 (2005).
12. K. Cvecek, K. Sponsel, R. Ludwig, C. Schubert, C. Stephan, G. Onishchukov, B. Schmauss, and G. Leuchs, "2R-regeneration of an 80-Gb/s RZ-DQPSK signal by a nonlinear amplifying loop mirror," *IEEE Photonics Technol. Lett.* **19**(19), 1475–1477 (2007).
13. K. Sponsel, K. Cvecek, C. Stephan, G. Onishchukov, B. Schmauss, and G. Leuchs, "Multilevel phase-preserving amplitude regeneration using a single nonlinear amplifying loop mirror," *IEEE Photonics Technol. Lett.* **19**(22), 1858–1860 (2007).
14. F. Wen, S. Sygletos, C. P. Tsekrekos, X. Zhou, Y. Geng, B. Wu, K. Qiu, and S. K. Turitsyn, "Multilevel power transfer function characterization of nonlinear optical loop mirror," in *19th International Conference on Transparent Optical Networks (ICTON)* (2017), paper We.D5.3.
15. Thorlabs, https://www.thorlabs.com/newgrouppage9.cfm?objectgroup_id=9567.
16. K. Zhou, D. J. Webb, C. Mou, M. Farries, N. Hayes, and I. Bennion, "Optical fiber cavity ring down measurement of refractive index with a microchannel drilled by femtosecond laser," *IEEE Photonics Technol. Lett.* **21**(22), 1653–1655 (2009).
17. L. E. Roberts, R. L. Ward, S. P. Francis, P. G. Sibley, R. Fleddermann, A. J. Sutton, C. Smith, D. E. McClelland, and D. A. Shaddock, "High power compatible internally sensed optical phased array," *Opt. Express* **24**(12), 13467–13479 (2016).
18. M. Sorokina, "Design of multilevel amplitude regenerative system," *Opt. Lett.* **39**(8), 2499–2502 (2014).
19. M. A. Sorokina and S. K. Turitsyn, "Regeneration limit of classical Shannon capacity," *Nat. Commun.* **5**(1), 3861 (2014).
20. J. Kakande, R. Slavík, F. Parmigiani, A. Bogris, D. Syvridis, L. Grüner-Nielsen, R. Phelan, P. Petropoulos, and D. J. Richardson, "Multilevel quantization of optical phase in a novel coherent parametric mixer architecture," *Nat. Photonics* **5**(12), 748–752 (2011).
21. S. Sygletos, P. Frascella, S. K. Ibrahim, L. Grüner-Nielsen, R. Phelan, J. O’Gorman, and A. D. Ellis, "A practical phase sensitive amplification scheme for two channel phase regeneration," *Opt. Express* **19**(26), B938–B945 (2011).
22. S. L. I. Olsson, H. Eliasson, E. Astra, M. Karlsson, and P. A. Andrekson, "Long-haul optical transmission link using low-noise phase-sensitive amplifiers," *Nat. Commun.* **9**(1), 2513 (2018).